Using the activity of naturally occurring radionuclides to identify the contribution of the Al industry to the atmosphere and plants

Laurent Pourcelot, Olivier Masson, Magali Beguin-Leprieur, Béatrice Boulet, Xavier Cagnat, Anne de Vismes-Ott, Azza Habibi, Hugo Jaegler, Christele Wampach Aubert, Daniele Dias Varela, et al.

Using the activity of naturally occurring radionuclides to identify the contribution of the Al industry to the atmosphere and plants

L. Pourcelot[1], O. Masson[1], M. Beguin-Leprieur[2], B. Boulet[3], X. Cagnat[3], A. De Vismes-Ott[3], A. Habibi[4], H. Jaegler[4], C. Wampach[4], D. Dias Varela[4], S. Fleury[4], F. Treille[4], P. Hennequet[4], J-M Métivier[1], C. Cossonnet[3*], J-C Raynal[5], Y. Noack[6]

[1]Institut de Radioprotection et de Sûreté Nucléaire IRSN/PSE-ENV/SEREN Cadarache, France
[2] Institut de Radioprotection et de Sûreté Nucléaire IRSN/PSE-ENV/SIRSE Le Vésinet, France
[3] Institut de Radioprotection et de Sûreté Nucléaire IRSN/PSE-ENV/SAME Orsay, France
[4] Institut de Radioprotection et de Sûreté Nucléaire IRSN/PSE-ENV/SAME Le Vésinet, France
[5]Aix-Marseille Université, CNRS, ECCOREV, Aix-en-Provence, France
[6]Aix-Marseille Université, CNRS, IRD, INRAE, Collège de France, CEREGE, Aix-en-Provence, France

Abstract

Alumina production from bauxite ore gives rise to a large amount of liquid and solid waste since the production of 1 kg of alumina involves the same weight of solid residue, the well-known red muds enriched in iron and heavy metals. Up to now, without any valorization of by-products, the red muds have been stored in artificial ponds which are a potential source of pollutants for the surroundings due to the uplift of red dust under strong wind conditions. The goal of the current work is to perform an in situ study of the transfer of red mud micro particles in the atmosphere and in the terrestrial environment around the red mud disposition basins. To this end, the activity concentration of NORM (Naturally Occurring Radioactive Materials such as ^{238}U, decay products and ^{232}Th) determined in plant leaves (*Quercus robur* and leaf vegetables) and in grains (wheat) is compared with the activity of the atmospheric micro particles, both taken in the environment of the red mud disposition basins (100 to 1,500 m). The activity ratios of NORM in vegetation and atmospheric micro particles are also compared to the ratios of potential sources of dust, such as soil and, above all, the red mud and bauxite emitted from the basins and from the piles, respectively.

The increase in ^{232}Th and ^{238}U activity concentration in a few tree leaves (by a factor of 9 and 4, respectively) and in some aerosol samples is accompanied by a decrease in ^{238}U/^{232}Th activity ratio for these matrices. Low ^{238}U/^{232}Th is also observed in bauxite and red mud. This suggests that the airborne particles emitted by bauxite piles and red mud basins first contaminate the atmosphere and then the leafs surfaces, after deposition. Locally-produced foodstuffs at a distance greater than 1,000 m from the ponds do not show any excess radionuclides, suggesting the low influence of airborne particles from the alumina production. Further variations in the ^{210}Po/^{210}Pb ratio in the plants and the atmospheric micro particles are consistent with the variation over time of these radionuclides coming in all likelihood from the atmosphere rather than from the aluminum industry.

[*] this work is dedicated to the memory of Catherine

1 Introduction

Industry remains an important source of environmental contamination in the air and terrestrial plants by heavy metals and metalloids which may pose a serious threat to ecosystems and the population (Geagea et al., 2008; Hissler et al., 2008; Zhang et al., 2009; Guo et al., 2012; Guéguen et al., 2012). Alumina production from bauxite ore gives rise to a large amount of liquid and solid waste since the production of 1 kg of alumina involves almost the same weight of solid residue, the so-called "red muds" characterized by extreme alkalinity (pH: 11-14), the presence of toxic elements (aluminum, iron and heavy metals) and NORM (Natural Occurring Radioactive Materials, such as ^{226}Ra, ^{230}Th and ^{210}Pb among others). Up to now, without any valorization of by-products, the red muds have been stored in artificial ponds, which are a potential source of pollutants for the surrounding environment. The collapse of tailing dams has induced several environmental disasters in Brazil and earlier in Hungary (Segura et al., 2016; Hatje et al., 2017). After the 2010 accident in Ajka (Hungary), both aquatic and terrestrial environments were affected, including rivers, agricultural lands, grasslands, woodland areas and human settlements.

In addition to accidental release, red mud disposition facilities remain a potential source of pollutants for nearby surroundings due to the uplift of red dust under strong wind conditions. Such a chronic emission pathway has been poorly studied to date and the terrestrial environment around red mud disposition ponds has not been studied. Apart from that, biomonitoring in the environment surrounding nuclear facilities followed by isotopic analyses was used to investigate the extent of the area influenced by chronic or accidental releases, in the absence of activities measured in the air (Bellis et al., 2001; Pourcelot et al., 2011; Tortorello et al., 2013; Conte et al., 2017). In such studies, the use of U-isotopes for environmental monitoring is based on the assumption that the isotopic composition of uranium released by the nuclear industry is known. A deep comparison of available environmental data (activity of biomonitors, edible plants and aerosols) in the environment of several nuclear facilities showed that ^{238}U activity in plants is influenced by the magnitude of waste released into the atmosphere (Pourcelot et al., 2017). In parallel to the attention paid to the environment influenced by anthropogenic releases, several works carried out on bioindicators and foodstuff taken at remote sites provide the radiological background (Anke et al., 2009; Rihs et al., 2011; Jeambrun et al., 2012). The determination of background activities in plants is crucial since it contributes to the estimation of the NORM potentially added to these matrixes by anthropogenic activities, namely, in the present study, the aluminum industry, whose main solid residue - the red muds - is potentially emitted in the atmosphere as micro particles. Thus, using the methodology already applied in the environment of nuclear facilities, the current work contributes to a deeper knowledge of the consequences of alumina production in the atmospheric and terrestrial environments. More precisely, it aims to qualify the main sources, whether natural (radiological background of the studied area) or anthropogenically-induced (mainly from bauxite piles and red mud ponds) using NORM. For these purposes, the current work compares the activity concentration of NORM (^{238}U and decay products as well as ^{232}Th) in plant leaves (Q*uercus robur* and leaf vegetables) and in grains (wheat) with those of aerosols and potential sources of atmospheric particles such as soil and, above all, dust emitted from the red mud ponds and bauxite piles, to better understand how the latter may influence activity levels in the air and in terrestrial plants. Thus, beyond representing an environmental monitoring study, the current work has a strong innovative character since it aims to trace the environmental impact of a non-nuclear industry, namely Al industry, using the activity of NORM determined in different compartments. Indeed activity ratios can be used to better constrain the influence of the main sources of NORM in the environment, namely atmospheric radionuclides and actinides from the aluminum industry.

2 Studied area, sampling and measurement methodologies

2.1 Studied industrial sites and sampling sites

Since 1894, the production unit of Gardanne (S of France) has produced alumina (Al_2O_3) from bauxite. Today alumina is mainly used in cosmetic and electronic components and before the 1990's, alumina was converted to aluminum. At the end of the manufacturing process, the solid residue is suspended in water and sent by pipe to the red mud disposition unit, located in Mange Garri about 2,500 m away from the alumina production unit (Figure 1). There, the solid phase is separated from the suspension liquid and sent to a dedicated dry disposition basin. Indeed, the waste disposal unit (total surface area: 28.5 ha) is divided into 7 disposition basins, two of which are actually in operation (Lasalle and Malfait, 2017). A total volume of 2,600,000 m^3 is available for waste disposal. The liquid phase is discharged off the Mediterranean coast, through a 61 km long pipe. In addition, bauxite, currently imported from Guinea, is stored in piles to the SE of the waste disposal unit at Mange Garri and thus constitutes another further source of atmospheric dust.

The prevailing wind, namely Mistral, comes from the NW (between 300° and 330°) (Météo-France data, Aix-en-Provence), about 5 km away from the studied site. It blows on average 55% of time and is characterized by high wind speeds up to 15 m s^{-1} hourly averaged. Another wind contribution comes from the opposite side (between 100 and 110°) (Figure 1). The activity concentration of natural radionuclides such as ^{238}U, some decay products, and ^{232}Th was determined in plants (tree leaves, lettuces and wheat grains) sampled in 2018-2019 at plots located 100 to 1,500 m downwind from the solid residues disposition area (Figure 1). For comparison, plant samples (three samples of oak tree leaves, one sample of wheat and one sample of leaf vegetables) were taken at sites out of the influence of, or remote from, the alumina production facility and the red mud disposition unit. Furthermore, atmospheric aerosols were taken east of the basins, in the city of Gardanne (sites AA05 and GAR, in 2015 and 2019, respectively) and west of the basins, in the city of Bouc-Bel-Air (sites AA01 and BBA, in 2015 and 2020, respectively).

Red muds and bauxite samples were also available and thereafter analyzed in order to characterize their potential influence in environmental samples: aerosols, biomonitors and locally-produced foodstuff. Prior to drying and radiological analyses, samples of red muds and bauxite were sieved (< 50 µm) to analyze the fraction as close as possible to that corresponding to the size distribution of atmospheric dust.

2.2 Aerosol sampling methods

Two aerosol sampling campaigns were conducted in 2015 and 2018-2020, each with a specific methodology (Table 1). In 2015, daily aerosol sampling was performed using a medium-volume sampler (80 m^3 h^{-1}) while in 2018-2020, weekly samplings were performed with a high-volume sampler (400 m^3 h^{-1}). In both cases, it was possible to investigate NORM activity over a relatively short period of time (6 weeks for the 2015 campaign) while the latest field campaign lasted several months. The main advantage of daily sampling was the possibility to differentiate between results according to an assumed steady state meteorological situation while weekly sampling most often corresponded to a range of different meteorological conditions. The main advantage of weekly sampling is to gather a sufficient amount of radionuclides on the filter to lower the uncertainty associated with the result, which is crucial regarding the interpretation of the activity or activity ratio. It also makes it possible to determine the ^{210}Pb level, which was not possible in 2015 due to an insufficient amount of ^{210}Pb in the filters. In both cases, aerosols were sampled using high collection efficiency filters (> 93% for submicron aerosols) to ensure the representativeness of the airborne size spectrum.

Table 1: Sampling methodologies used for atmospheric micro particles in 2015 and in 2018-2020.

Sampling years	***2015***	***2018-2020***
Sampling site locations with respect to the red mud disposition unit	AA05: 1,500 m E AA01: 500 m W	GAR: 1,600 m E BBA: 400 m W
Duration of observation (weeks)	AA01: 3 AA05: 2.5	GAR: 40 BBA: 8
Duration of sampling (days)	1	7
Sampling rate (m^3 h^{-1})	60	400
Number of available filters	AA01: 22 AA05: 17	GAR: 39 BBA: 7

Table 2: Local foodstuff samples taken in the environment of a red mud disposition unit.

sample		***location: direction and distance to the red mud disposition unit***	***sampling date***	***weight (kg fresh matter)***
BMP6	lettuce	1,500 m west	28/06/2018	2.5
BMP7	lettuce	2,500 m east	26/07/2018	2.3
BMP9	lettuce	4,000 m south	26/07/2018	0.9
BMP11	chard	1,400 m east	28/08/2018	5.1
BMP12	cabbage	1,400 m east	28/08/2018	0.5
BMP1	wheat	1,200 m SE	27/06/2018	5.1
BMP3	barley	1,200 m west	27/06/2018	4.2
BMP5	wheat	7,500 m north	27/06/2018	2.9

2.3 Vegetal and soil sampling methods

Sixteen samples of tree leaves (Q*uercus robur)* were taken in October 2018 and October 2019, using the same methodology. About 5 kg of leaves was separated by hand from branches cut at heights varying from 1.5 to 3 m above the ground. Local foodstuffs such as wheat grains and leaf vegetables were taken at maturity in the fields or in gardens, respectively. The main difficulty regarding foodstuff is their availability over the study period, and thus the number of samples is limited to three samples of wheat grains and five samples of leaf vegetables. Unfortunately, it was not possible to focus sampling on a single foodstuff. Thus, two common species of cereals were taken such as 'winter wheat' (*Triticum turgidum* sp.) and barley (*Hordeum vulgare* sp.). In addition, the term 'leaf vegetables' refers to three edible species each characterized by a specific capitation surface and a specific biomass: lettuce, cabbage and chard. Furthermore, the available mass for radiological analyses varies substantially (Table 2). Thus 2.9-5.1 kg of wheat grain was easily reached, whereas the mass of leaf vegetables varies from one plot to another according to availability, from 0.5 to 5.1 kg per sample.

In addition to foodstuff, five cultivation soil samples were taken toward 0.1 m deep, using a stainless drill corer of 8 cm diameter.

Back to the laboratory and before drying at 105 °C, samples were sorted to remove any undesirable materials. Leaf vegetable samples were washed with deionized water. Non-husked wheat and barley grains were analyzed. Soil samples (about 2 kg each) were homogenized using a spoon, sieved to remove coarse material (> 2 mm) and thereafter dried at 80 °C for five days.

2.4 Analytical procedures

Three techniques have been used according to each radionuclide: (*1*) gamma spectrometry is used to quantify the activity of decay daughters of ^{238}U (namely ^{234}Th, ^{226}Ra, ^{214}Pb, ^{214}Bi and ^{210}Pb), (*2*) inductively coupled plasma mass spectrometer (thereafter ICP-MS) is used for uranium (^{234}U and ^{238}U) and thorium isotopes (^{232}Th and ^{230}Th), finally (*3*) alpha spectrometry

is used to determine ^{210}Po activity. The analytical methods used are validated each year by participating in different worldwide proficiency tests and are used in the framework of routine environmental sample analyses.

2.4.1. Gamma spectrometry

Prior to gamma spectrometric measurements, the dry plant samples were first reduced to ash (480 °C for 52 h). Then the ashes were ground and compacted in a 60 mL cylinder box. Dry samples of soil, bauxite and residue were also ground and compacted in a 60 mL cylinder box. These boxes were then vacuum-packed in airtight packets in order to conserve ^{222}Rn and keep the same measurement geometry. Measurements were performed at least 24 days after packaging, which is the required time period for the decay products of ^{226}Ra to reach equilibrium. Indeed, after this delay, corresponding to more than six half-lives of ^{222}Rn, the activity of this radionuclide is close to 99% of ^{226}Ra activity, and therefore it can be assumed that equilibrium has been reached.

Gamma spectrometry was performed by counting for 80,000 s using hyper-pure germanium (HPGe) detectors with a relative efficiency greater than 50% (BEGe detectors from Canberra, or Profile-FX detectors from Ortec). These new-generation detectors exhibit better resolution and a lower background than coaxial n-type HPGe detectors. This type of gamma spectrometry can be used to determine ^{234}Th, ^{226}Ra, ^{214}Pb, ^{214}Bi and ^{210}Pb (daughters of ^{238}U). The ^{226}Ra activity determined by gamma spectrometry is associated with a large uncertainty, but ^{214}Bi and ^{214}Pb measurements can be used to evaluate the distribution of ^{226}Ra in plants.

The decision threshold for plant and soil samples is 1 Bq kg^{-1} of ash for ^{214}Pb and ^{226}Ra, 5 Bq kg^{-1} of ash for ^{234}Th and 0.002 to 1 Bq per filter in aerosol samples.

2.4.2 Inductively coupled plasma mass spectrometer

Dry samples of plants, soils, bauxite and red muds were first reduced to ash (480 °C for 52 h). About 0.5 g of ash was taken for the analysis. A first digestion step was performed using the microwave system (Multiwave 3000, Anton Paar) with a mixture of concentrated acids (HNO_3, HCl and HF). The temperature was ramped to 240 °C over 60 min and then held constant for 30 min. Acids were then evaporated with the microwave system at 110 °C. Finally, a last microwave cycle was run in an $Al(NO_3)_3$ and 3 M HNO_3 solution in order to obtain the appropriate loading media for the chromatographic resin. The digested sample was then loaded on a 1.5 mL UTEVA resin, previously conditioned with 3 M HNO_3. After washing the resin with 3 M HNO_3, the Th fraction was eluted with 5 M HCl and then the U fraction with 0.01 M HCl. To control the flow rates from the resin, the bottom of the column was connected with a peristaltic pump (IP High Precision Multichannel Pump, Ismatec®). The optimal speed setting for the pump in our configuration was 52 rpm (rotations per minute) for the conditioning and the elution steps (about 3 mL min^{-1}) and 26 rpm (about 1.5 mL min^{-1}) for loading the sample and washing the matrix.

For aerosol samples, the first step was to ash the filters at 520 °C for 12 hours. An automated alkaline fusion was used to digest the samples by adding 3.5 g of $LiBO_2$ - LiBr (98.5% - 1.5%) to the ashes. The mixture was heated at 1000 °C for 15 min. The melt obtained was then transferred to a PTFE beaker containing 100 mL of 3 M HNO_3. Uranium and thorium were then coprecipitated with $Ca_3(PO_4)_2$ in order to eliminate some of the matrix components. After dissolving the precipitate in 6 M HNO_3, the silicon was eliminated by flocculation in order to prevent clogging in the system, by adding Polyethylene glycol 6000 to the sample. The precipitate was eliminated and $Al(NO_3)_3$ added to the solution. Uranium and thorium were purified using the UTEVA resin (Triskem, France) as described above for the plant and soil samples.

The acids used for radiochemistry (mineralization, purification) were Suprapur® grade, which is a good compromise between the price of the reactants and the addition of impurities to the sample. In addition, the amount of impurities is controlled with “blank analysis” (Table 3). For dilutions before the measurement by ICP-MS, Ultrapure grade of HNO_3 is used.

Table 3: Examples of measurement of blanks (HNO_3 Ultrapure, blank aerosol filter, i.e. without sampling) and aerosol filter (in cps: count per second). RSD: Relative Standard Deviation.

	m/z	229	230	232	233	234	235	236	238
HNO_3 - Ultrapure grade	average (cps)	0.1	0.1	2.5	2.9	2.0	2.3	0.9	25.0
	RSD (cps)	0.1	0.1	0.2	0.2	0.7	0.2	0.4	0.2
Blank aerosol filter spiked with Tracer solution ($^{229}Th/^{233}U$)	average (cps)	1398.6	6.6	10993.4	11448.2	6.7	153.7	0.21	21031.0
	RSD (cps)	46.4	1.7	1959.2	91.7	0.8	4.5	0.26	94.1
Aerosol filter with Tracer solution ($^{229}Th/^{233}U$)	average (cps)	236.9	15.8	3355767.1	8633.2	32.0	3621.5	0.2	507188.2
	RSD (cps)	2.7	0.9	25860.7	49.7	1.3	49.2	0.3	2463.7

Isotopic measurements of uranium and thorium were performed by inductively coupled plasma quadrupole-based mass spectrometer ICP-QMS (X Series 2, ThermoFisher Scientific). The sample was introduced into the ICP-MS with a classical concentric nebulizer (Meinhard® or Arimist®, 650 µL min^{-1}) and a Peltier cooled cyclonic spray chamber (2 °C). All ICP-MS data were acquired in electrostatic scanning and peak-jumping mode. The $^{235}U/^{238}U$ ratio of a certified reference material (CRM U030-A, NBL) was measured between every two samples in order to calculate the mass bias factor and to apply a correction according to the linear model. The specific activity of U and Th isotopes was calculated respectively from the responses of internal standards (^{233}U and ^{229}Th) added at the beginning of sample preparation, with the isotopic dilution method. Chemical yields according to the analysis were between 80-100% for U and 70-90% for Th. Measurements of blank samples, presented in table 3, show a low background of uranium isotopes in acid and in a blank aerosol filter.

For quality control purposes, a blank sample and certified reference materials were regularly analyzed. The results of IAEA 385 and NIST SRM 4359 reference materials are in good agreement with the certified values, with a standard deviation (namely E_n number) below one (Table 4). E_n number is calculated using equation [1]:

$$E_n = \frac{|A_1 - A_2|}{\sqrt{U_1^2 + U_2^2}} \qquad \text{Equation [1]}$$

In equation [1], A and U stand for the determined activity and the uncertainty of activity (2 sigma), respectively. Subscripts 1 and 2 refer to two different tests of the same reference material.

Table 4: Reference material analyses of U and Th isotopes. A and U_A are the activity concentration (Bq kg^{-1}) and the uncertainty at 2 sigma error (Bq kg^{-1}), respectively. E_n (dimensionless) is the standard deviation calculated using equation [1] (see text).

Standard Reference materials	radionuclides massic activities	^{234}U A (Bq.kg^{-1})	^{234}U U_A (k=2) (Bq.kg^{-1})	^{234}U En	^{238}U A (Bq.kg^{-1})	^{238}U U_A (k=2) (Bq.kg^{-1})	^{238}U En	^{230}Th A (Bq.kg^{-1})	^{230}Th U_A (k=2) (Bq.kg^{-1})	^{230}Th En	^{232}Th A (Bq.kg^{-1})	^{232}Th U_A (k=2) (Bq.kg^{-1})	^{232}Th En
IAEA-385	*certified values*	27.2	1.2		29.4	1.2		31.8	1.4		33.8	0.9	
sediment	**sample test 1**	28.7	3.6	**0.40**	30.2	3.1	**0.24**	32	11	**0.02**	35.8	5.8	**0.34**
	sample test 2	27.8	3.5	**0.16**	29.3	2.9	**0.03**	34	11	**0.20**	34.3	5.7	**0.09**
NIST SRM 4359	*certified or informative* values*	9.5	1.1		8.67	0.54		3.3	1.65	*	2.4	0.30	
seaweed	**sample test 1**	9.2	1.1	**0.20**	8.33	0.82	**0.35**	3.4	1.1	**0.05**	2.48	0.41	**0.16**
	sample test 2	8.6	1.1	**0.58**	7.75	0.77	**0.98**	3.5	1.3	**0.10**	2.89	0.47	**0.88**

Limit of quantification is 0.1 Bq kg^{-1} of ash for ^{230}Th, 0.03 Bq kg^{-1} for ^{232}Th and 0.2 Bq kg^{-1} for ^{234}U and ^{238}U.

2.4.3. Alpha spectrometry

Alpha spectrometry is used to determine ^{210}Po activity. After the acidic dissolution of dried samples, the solution is evaporated until dry and the residue is dissolved with 6 M hydrochloric acid. In this medium, the metallic form of polonium is spontaneously deposited on stainless steel plates by reduction. The deposited polonium is then quantified by alpha spectrometry using ^{209}Po as a tracer. Measurements are performed using Passivated Implanted Silicon Detectors (PIPS) placed in a vacuum chamber, with a distance of 13 mm between the detector and the source. These detectors have a 600 or 900 mm^2 active area. Alpha source stainless steel plates are counted by alpha spectrometry for approximately 69 hours.

Decision threshold for ^{210}Po activity is 0.25 Bq kg^{-1} of dry material.

2.4.4. Units for NORM activity concentration

The concentration activity of radionuclides, decay-corrected to the dates of sampling, is expressed in µBq m^{-3} in aerosol samples, in Bq kg^{-1} of dry material in bioindicators and in Bq kg^{-1} of fresh material in foodstuff (grains and leaf vegetables). All results are given in specific tables (see tables s1 to s5 in Supplementary Material). In all cases, the uncertainty of activity is 2 sigma errors.

3 Results

This paragraph aims at better understanding the transfer of red mud particles in the surroundings of the basins, namely in the atmosphere and in plants using NORM signatures. Thus, the activity of NORM measured in the potential sources of radionuclides (soil, bauxite and red mud) is presented first. Then the NORM activity recorded by aerosols, considered as the atmospheric vectors of dust, is shown and finally the NORM activity in terrestrial plants (tree leaves and terrestrial foodstuff), considered as the receptors of atmospheric dust, is presented. In addition, the actinides in the environmental samples are compared to actinides in the potential sources in order to evaluate the influence of the Al industry on the environment.

3.1 NORM activity in soil, bauxite and red mud

Soil concentration activity barely varies between radionuclides. Thus, radionuclides belonging to the ^{238}U decay chain may be considered in secular equilibrium (see table S1 in the Supplementary Material, Figure 2). Surprisingly, no enrichment in ^{210}Pb of atmospheric origin with respect to radioactive precursor is noticeable. Whatever the soil sample considered, both primordial radionuclides ^{232}Th and ^{238}U exhibit the same level of concentration activity. The variation in concentration activity from sample to sample remains low, less than a factor two whatever the radionuclide considered. For example, the concentration activity of ^{232}Th ranges between 27±5 and 42±7 Bq kg^{-1}.

Both red mud and bauxite samples exhibit higher concentration activity than soil samples. In bauxite and red mud the concentration activity of ^{238}U is 83±8 and 189±19 Bq kg^{-1} respectively, whereas it ranges between 20±2 and 34±3 Bq kg^{-1} in soil. Especially in the red mud, radionuclide concentrations are four to nine times higher than in soil and more than two times higher than in the bauxite. These observed activity ratios between red muds and bauxite, 2.3 for both ^{238}U and ^{232}Th, are the same as the enrichment factors of waste compared to the raw material (Goronovski et al., 2019).

Almost no variation in activity occurs along the ^{238}U-decay series, implying that the radionuclides reached secular equilibrium whatever the raw or the waste material considered. This observation is rather astonishing, since red mud, the solid residue of intense alkaline leaching of bauxite, does not record any depletion of the most soluble radionuclides, removed with the liquid phase or enrichment of the most refractory radionuclides (such as ^{230}Th).

Both anthropogenic materials (raw material and solid residue) are characterized by higher ^{232}Th concentration activity (185±30 and 241±23 Bq kg^{-1} respectively) with respect to ^{238}U (83±8 and 189±19 Bq kg^{-1} respectively). Indeed, bauxite is

characterized by NORM concentration activity close to or above 100 Bq kg^{-1}, with higher ^{232}Th (185±3 Bq kg^{-1}) than ^{238}U concentration activity (95±5 Bq kg^{-1}) and thus $^{232}Th/^{238}U$=0.5 significantly below one (Karagiannidi et al 2009).

Hence, the influence of dust deriving from bauxite or red muds with $^{232}Th/^{238}U$=0.4±0.1 is distinguishable from the dust emitted by soil, characterized by the same level of ^{232}Th and ^{238}U and therefore with an activity ratio close to one. In addition, the soil, which does not show any excess ^{232}Th with respect to ^{238}U, is not influenced by the aluminum industry.

3.2 NORM activity in atmospheric micro-particles

This paragraph aims to identify any influence of the aluminum industry in the low atmosphere surrounding the facility using NORM activity.

Considering the radionuclides studied, ^{210}Pb exhibits by far the highest volume activity, ranging between 152±14 and 2050±250 µBq m^{-3} (see tables s2 and s3 in the Supplementary Material, Figure 3). Samples taken in 2015 east and more particularly west of the red mud disposition unit exhibit higher ^{210}Pb (on average 840 and 1178 µBq m^{-3} respectively) than the average value obtained in 2018-2020 (East: 621 µBq m^{-3} and West: 529 µBq m^{-3}).

For samples taken in 2018-2020, the volume activity of ^{210}Po is also available. This radionuclide exhibits a lower mean activity (8.3 µBq m^{-3}) than its radioactive parent (mean ^{210}Pb: 621 µBq m^{-3}) (Figure 3). The observed $^{210}Po/^{210}Pb$ ratio ranging from 0.003 to 0.04 is consistent with the ratio usually reported in the lower atmosphere (Baskaran, 2011).

Compared to ^{210}Pb, actinides from the ^{238}U decay chain and ^{232}Th show lower activity levels. For instance, the ^{238}U volume activity ranges between 0.2±0.02 and 2.5±0.3 µBq m^{-3}. Thus, with the exception of ^{210}Pb and ^{210}Po, ^{238}U and available decay products (^{234}U and ^{230}Th) are at secular equilibrium.

Samples taken E and W of the waste disposal pond during the two different campaigns (2015 and 2018-2020) recorded activity of the same order of magnitude whatever the actinide considered, however the mean activity values measured in 2015 are higher to the mean values of 2018-2020 (Figure 3). Hence the data set of 2015 has caught our attention with activity of ^{232}Th or ^{238}U exceeding 2 µBq m^{-3} for four samples. Despite a higher number of samples in 2018-2019 (39 samples in Gardanne), no volume activity exceeding this level was observed, probably because of the sampling duration, *i.e.* one week *vs* one day in 2015 which may have smoothed out variability. Therefore, it may be supposed that several meteorological conditions affected one week of sampling, with the resulting activity considered as a 'mean', while in comparison a daily sample corresponds to one single meteorological condition and hence may highlight some specific and favorable conditions for dust particle emission and transport.

Day-to-day variation in volume activity shows that actinides are further characterized by higher variability (defined as the ratio between the standard deviation and the mean: 90% and 110% for ^{238}U and ^{232}Th respectively) compared to ^{210}Pb (40%) (Figure 4-a). An in-depth analysis of the highest actinide activity shows that those samples are characterized by higher ^{232}Th with respect to ^{238}U, in other words by $^{238}U/^{232}Th$ reaching 0.6±0.1, whereas the mean activity ratio was 1.1 in 2015.

In comparison, narrow variations in the volume activity of ^{232}Th and ^{238}U are observed in 2018-2020, with variability of 61 and 51%, respectively (Figure 4-b). Consequently, the weekly $^{238}U/^{232}Th$ activity ratio remains close to the mean value (1.1) and no deviation toward lower ratios is especially noticeable in this set of data.

Hence, the few samples of atmospheric micro particles taken in 2015 characterized by the lowest $^{238}U/^{232}Th$, with the highest ^{232}Th volume activity, are closer to the ratio of red muds and bauxite (0.4±0.1).

In addition, it is noteworthy that three of the four of the samples characterized by enhanced ^{232}Th and low $^{238}U/^{232}Th$ show the highest ^{210}Pb activity (above 1400 µBq m^{-3}) that accounts for the elevated mean activity (1178 µBq m^{-3}) underlined above. Thus, the influence of airborne particles from the Al industry is suspected in some of the atmospheric samples based on the actinide signature and also the slight enhancement in ^{210}Pb volume activity.

3.3 NORM activity in plants

In this paragraph, we use the activity of NORM to check if the aluminum industry also contributes to the contamination of terrestrial plants. In this respect, close attention has been paid to the actinide content of terrestrial plants since actinides were shown to be tracers of atmospheric dust deriving from the aluminum industry in the previous paragraph. The activity of NORM in local foodstuffs is further compared to activity previously measured at remote sites, in order to confirm the lack of impact on local foodstuffs as suggested by the actinides.

Oak tree leaves

Oak tree leaves exhibit large variations between radionuclides (see table s4 in the Supplementary Material). Thus, radionuclides whose source is dominated by the atmosphere, such as ^{210}Po and ^{210}Pb, exhibit by far the highest activity (several ten Bq kg^{-1}) and narrow variability (40%). Such high activity supports the importance of ^{210}Pb deposition from the atmosphere produced from the decay of ^{222}Rn (Sheppard et al., 2008).

The relative importance of foliar *vs* root uptake of these radionuclides is mainly justified by the low concentration of NORM in soil, as underlined in the previous section. Above all, experimental data showed that atmospheric deposition is the main source of ^{210}Po and ^{210}Pb in the aboveground parts of plants (Pietrzak-Flis and Skowrońska-Smolak, 1995). In the tree leaves studied, the mean ^{210}Po/^{210}Pb activity ratio of 1.4 with a variability of 20% is close to the ratio given in the review of Sheppard et al. (2008) (0.4 to 1.5). The influence of ^{210}Po or ^{210}Pb from bauxite or red mud must be discarded since the latter, unlike oak leaves, do not exhibit any enrichment in those radionuclides with respect to other ^{238}U decay products.

The concentration activity of ^{226}Ra (and its short radioactive period decay products ^{214}Pb and ^{214}Bi, in equilibrium with ^{226}Ra) in oak leaves (a few Bq kg^{-1}) is by far higher than the activity of actinides, i.e. uranium and thorium isotopes (^{238}U, ^{234}Th, ^{234}U, ^{230}Th and ^{232}Th) whose activity lies close to or below 1 Bq kg^{-1}. Similarly to ^{210}Pb and ^{210}Po, the influence of ^{226}Ra from bauxite or red mud must be discarded since the latter, unlike oak tree leaves, do not exhibit any enrichment in ^{226}Ra with respect to other ^{238}U decay products.

In tree leaves, the variability of concentration activity for each radionuclide (defined as the ratio between the standard deviation and the mean) of ^{226}Ra (36%), ^{210}Po, ^{214}Pb, ^{214}Bi (32%) and ^{210}Pb (35%) is almost the same. For these radionuclides, the same range of activity is further observed between samples taken in the environment of the waste disposal unit (whether W or E) and samples taken out of the influence of the study site (see table s4 in the Supplementary Material). These arguments suggest that ^{210}Pb, ^{210}Po, ^{226}Ra as well as ^{214}Pb and ^{214}Bi determined in the tree leaves are not suitable tracers of the atmospheric dust emitted by bauxite piles and red mud basins.

By contrast, the low concentration activity of actinides in tree leaves (in most cases below 1 Bq kg^{-1}) makes these tracers particularly sensitive to any atmospheric inputs. Indeed, with respect to the previously discussed radionuclides, a higher variability in actinides is observed: variability of ^{238}U and especially of ^{232}Th reaches 64% and 92% respectively. Furthermore, the resultant map reveals spatial variation of ^{232}Th, with the highest activity recorded a few tens of meters east from the edge of the disposal unit studied (1.3±0.2 and 1.6±0.3 Bq kg^{-1}) (Figure 5). When the distance increases (1,000 to 1,500 m), the concentration activity of ^{232}Th decreases: 0.3±0.06 to 0.8±0.1 Bq kg^{-1} on the eastern side and 0.2±0.04 to 0.3±0.04 Bq kg^{-1} on the western side. This latter range is close to the level of activity in leaf samples taken away and remote from red mud disposition units (^{232}Th: 0.1±0.02 to 0.2±0.04 Bq kg^{-1} in the present study and 0.2 Bq kg^{-1} according to Carvalho et al., 2014 and Pourcelot et al., 2017).

Interestingly, tree leaf samples exhibiting the highest ^{232}Th activity (above 0.5 Bq kg^{-1}) are further characterized by low ^{238}U/^{232}Th activity ratio below one (0.8-0.7), whereas on the opposite side samples taken away from the aluminum industry

influence are characterized by both low ^{232}Th and high ^{238}U/^{232}Th ratios, far above one. Thus, the lowest ^{238}U/^{232}Th ratio together with higher ^{232}Th levels in a few samples taken in the close vicinity of the study site suggest a potential influence of red muds for which the ^{238}U/^{232}Th ratio reaches 0.4±0.1, as shown in section 3.1.

Contrary to atmospheric aerosols (previous section), none of the tree leaf samples exhibiting enhanced ^{232}Th activity are concomitantly characterized by enhanced ^{210}Pb activity.

Wheat grains

As for oak tree leaves, wheat grain activity varied significantly between radionuclides, with the highest values for ^{210}Po and ^{210}Pb (5.1±0.5 to 7.0±0.7 Bq kg^{-1} for the latter), intermediate values for ^{226}Ra and decay products (^{214}Pb and ^{214}Bi: 0.2±0.05 to 0.6±0.08 Bq kg^{-1}) and the lowest ones for actinides (see table s5 in the Supplementary Material). Thus, the activity measured in wheat grains emphasizes the role played by the deposition of radionuclides from the atmosphere (for ^{210}Po and ^{210}Pb) and root uptake from soil (for ^{226}Ra) in the activity recorded by terrestrial plants. A mean activity ratio ^{210}Po/^{210}Pb of 0.4 is due to an excess of ^{210}Pb with respect to ^{210}Po in the three available samples.

Higher variability is observed for each U or Th isotope (50-60%) than for ^{210}Pb or for ^{210}Po (20-30%), again suggesting that each U or Th isotope is a sensitive indicator of the atmospheric inputs onto plant surface. Thus, actinides vary from one sample to another, with higher activity in sample BMP1 taken east of the waste disposal unit, with 0.05±0.01 and 0.06±0.01 Bq kg^{-1} of ^{238}U and ^{232}Th respectively compared to sample BMP3 taken west with 0.02±0.002 and 0.02±0.003 Bq kg^{-1} of ^{238}U and ^{232}Th respectively. However, wheat data do not allow us to conclude the influence of actinides emitted by the study sites, since the sample taken at a remote distance from the studied site (BMP5 7,500 m NE) exhibits intermediate actinide activity *i.e.* between the activities of the samples taken east and west of the study site. Above all, unlike some tree leaf samples taken in the close vicinity of the waste disposal unit, no significant enrichment in ^{232}Th with respect to ^{238}U is observed in wheat grains.

Leaf vegetables

The concentration activity of NORM in leaf vegetables is lower than in wheat grains, with activity well below 1 Bq kg^{-1}, whatever the radionuclide considered (see table s5 in the Supplementary Material, Figure 6). As expected, ^{210}Pb (from 0.2±0.06 to 1.0±0.1 Bq kg^{-1}) and to a lesser extent ^{210}Po (from 0.09±0.02 to 0.3±0.06 Bq kg^{-1}) exhibit the highest concentration activity. The mean ^{210}Po/^{210}Pb activity ratio reaches 0.4, due to an excess of ^{210}Pb with respect to ^{210}Po.

Only slight variation in ^{226}Ra (and decay products) occurs among samples (a factor of about four) with respect to variation in actinides, which reaches a factor of about fourteen. In detail, two groups of samples can be distinguished according to the actinide and ^{226}Ra concentration activities: *(1)* samples BMP6, BMP7 and BMP11 exhibiting higher ^{226}Ra (or ^{214}Pb and ^{214}Bi) (0.04±0.02 to 0.1±0.01 Bq kg^{-1}) than actinides (0.005±0.0005 to 0.02±0.002 Bq kg^{-1}), as previously observed in oak leaves and in wheat grains, *(2)* with samples 9 and 12, exhibiting higher levels of activity of actinides (0.06±0.006 and 0.1±0.01 Bq.kg^{-1}) compared to group (*1*) although ^{226}Ra has only slightly increased.

Although the species of leaf vegetable may account for a part of the previously-reported variability in actinides, available data are insufficient to understand the influence of the species of leaf vegetable on the concentration activity. However, the distribution of NORM in some of the samples with the same levels of actinides and ^{226}Ra named (*2*), similar to the distribution in the soil (no fractionation among ^{238}U decay products and same level of ^{238}U and ^{232}Th), suggests the potential contamination of leaves by soil particles, despite washing prior to radiological analyses.

As expected, the closest samples to the study site (BMP12 and BMP11, situated only 1,500 E of the site) show some of the highest NORM content. However, the sample taken furthest from the study site (BMP9, 4,000 m S), representative of the background level for leaf vegetables, records activity lying between those of BMP12 and 11. None of the samples taken E and

W from the study site (BMP6, 7, 11 and 12) exhibits excess ^{232}Th with respect to ^{238}U, noticeable in red muds, bauxite, some of the atmospheric particles and tree leafs samples (see previous sections). Thus, actinide activity suggests that the aluminum industry has no influence on the leaf vegetable samples.

No impact on cereals and leaf vegetables suggested by the $^{238}U/^{232}Th$ ratio is reinforced by the comparison with the specific activity of foodstuffs from other parts of the country (Figure 7). Indeed, the current activity of each radionuclide ranges between the lowest and highest values measured by Jeambrun et al. (2012), who used the same sampling methodology as us. However, grain activity from the current work is higher than the mean activity measured in other European countries (^{238}U: 0.011 Bq kg^{-1}, ^{230}Th: 0.016 Bq kg^{-1}, ^{226}Ra: 0.09 Bq kg^{-1}, ^{232}Th: 0.02 Bq kg^{-1}) because the grains were cleaned with distilled water and presumably husked before analyses (Pietrzak-Flis et al., 1997; Lindahl et al., 2011). Indeed, husking the wheat significantly reduces the activity of NORM in the remaining grains, whereas the husk retains most of the activity (Pourcelot et al., 2015). For the same reason, average ^{210}Pb concentration activities in wheat (0.20 Bq kg^{-1}) and barley (0.34 Bq kg^{-1}) given by previous works (McDonald et al., 1999; Turtiainen et al., 2011) are much lower than the average found in the present study (6.1 Bq kg^{-1}). However, despite such a difference due to sampling methods, $^{210}Po/^{210}Pb$ from the present work (0.3-0.5) is similar to activity ratios for samples from Canada (0.3-0.7) and the UK (0.08-1.08) with slightly accentuated ^{210}Pb activity with respect to ^{210}Po (McDonald et al., 1999; Sheppard et al., 2008).

In the current work, the variation of some of the radionuclides like ^{238}U, ^{230}Th or ^{210}Pb indeed exceeds that observed for leaf vegetables taken at country scale. As observed before, two of the samples exhibiting the highest actinide concentration activities and showing no fractionation between ^{238}U decay products, are suspected of contamination by soil particles. Such an unexpected influence of soil accounts for the large variability in activity for leaf vegetables.

4. Discussion

Comparing the concentration activity and activity ratios for NORM in terrestrial plants with those from the other compartments studied (soil, bauxite, red mud and aerosols) can be used to better constrain the influence of the potential radionuclide sources (radionuclides of atmospheric origin, radionuclides from soil or radionuclides emitted by the red muds disposition unit) in tree leaves and in foodstuff. Hence the influence of the aluminum industry on plants and aerosols manifests itself by the enhancement of the activity of actinides with respect to remote sites and by a low $^{238}U/^{232}Th$ activity ratio, close to that of bauxite and red mud (section 4.2). Further variability in the $^{210}Po/^{210}Pb$ activity ratio is noticeable in the samples of plants, which is explained by the influence of the atmospheric source (section 4.1).

4.1 Radionuclides of atmospheric origin

The plants studied show a regular trend when $^{210}Po/^{210}Pb$ is plotted versus the concentration activity of ^{210}Pb, suggesting a mixing of both radionuclide origins, each characterized by a specific ratio (Figure 8-a). Thus, oak tree leaves exhibit the highest ratio, close to secular equilibrium and with the highest concentration activity (23-63 Bq kg^{-1}), whereas, on the opposite side leaf vegetables have the lowest ratio (0.3-0.5) and lowest concentration activity. Compared to plants, the atmospheric particles witness an even weaker activity ratio (0.003-0.04) whereas secular equilibrium between ^{210}Pb and ^{210}Po is usually assumed for soil (Ekdal et al., 2006; Sheppard et al., 2008; IAEA, 2017). Hence from this comparison, radionuclides deriving from the atmosphere and from the soil appear as the two end members of the mixing trend, with vegetal samples more or less influenced by them.

Thereafter, the field data are compared to the activity ratio calculated for the atmosphere-derived radionuclides after deposition. For this calculation, we took into account the annual atmospheric deposition flux of ^{210}Pb in the area studied, given by the average value over the western Mediterranean area, namely 75 Bq m^{-2} y^{-1} (Garcia-Orellana et al., 2006). From

this value, we assumed a steady atmospheric deposition of ^{210}Pb all year long, i.e. 6.25 Bq month^{-1}. The proportion of ^{210}Po deposited is given by the mean ^{210}Po/^{210}Pb ratio of 0.01 in the atmospheric micro-particles obtained in the present study. We assumed no fractionation between ^{210}Po and ^{210}Pb during deposition and, after deposition, no weathering of radionuclides. Iterative calculation is then carried out, which involves both constant monthly deposition and the decay/ingrowth of radionuclides with time (namely ^{210}Pb, ^{210}Bi and ^{210}Po with a radioactive period of 22.3 y, 5 d and 138.4 d, respectively). We used equation [2] to calculate variation in ^{210}Po activity over time (t) (IAEA, 2017):

$$^{210}Po = {}^{210}Po0\left[1.0179\, e^{\lambda_{210Pb}t} + 0.037e^{\lambda_{210Bi}t} - 1.0555e^{\lambda_{210Po}t}\right] \qquad \text{Equation [2]}$$

In equation [2], $^{210}Po_0$ stands for the initial (t=0) activity of ^{210}Po; λ_{210Pb}, λ_{210Bi} and λ_{210Po} are the decay constants of ^{210}Pb (8.5E-05 d^{-1}), ^{210}Bi (1.4E-01 d^{-1}) and ^{210}Po (5.0E-03 d^{-1}), respectively.

From this assessment, a large variation in the ^{210}Po/^{210}Pb ratio (0.01-0.3) is observed after deposition and during the period of observation (6 months), meaning that a surface accumulating atmospheric deposits during several months is likely to show variation in the activity ratio with time exceeding one order of magnitude (Figure 8-a). Plant samples exhibit a similar variation (one order of magnitude between leaf vegetables and oak tree leaves) even if the actual plant ratios are somewhat higher than the calculated ones. Such a discrepancy between plant values and calculated deposition may be due to the ratio of the atmospheric source chosen for the calculation (^{210}Po/^{210}Pb=0.01) whose maximum reaches 0.04 (see section 3.2). Thus, the variation in the activity ratio in plant samples mimics the variation in atmospheric deposits with time, suggesting that the ratio recorded by leaves varies with the period of exposure to the atmosphere. Hence, leaf vegetables, whose growth time is about one month, have the lowest ratio whereas oak tree leaves, which have been exposed to atmospheric deposition for about six months have the highest ratios. The intermediate signature of wheat grains is consistent with 2-3 months of exposure, which is approximately the growing time of grains. Thus, in spite of a large gap between plant ratios and atmospheric particles, the ^{210}Po/^{210}Pb ratio of the vegetal samples is consistent with variation over time for these radionuclides from the atmosphere.

4.2 Tracing the influence of the aluminum industry using actinides

The large variation in the ^{238}U/^{232}Th activity ratio in plants reported in previous sections is plotted against ^{232}Th activity (Figure 8-b). Indeed, as underlined in section 3.3, the strongest variations are noticeable for oak tree leaves, with remote samples characterized by a lower activity and a higher ratio, whereas samples taken close to the red mud disposition unit show the lowest ratio (down to 0.7) and the highest ^{232}Th activity. Narrow variation in this ratio is observed for foodstuff whose lowest value remains close to 0.9 and ^{232}Th below or about 0.1 Bq kg^{-1}. It is noteworthy that the tree leaf ratio mimics variation in atmospheric particles and especially samples taken in 2015, suggesting that the actinides measured in tree leaves originate from low atmospheric dust. Considering the samples studied, bauxite and red muds record the lowest ratio (^{238}U/^{232}Th = 0.4), suggesting that such anthropogenic materials are a significant source of actinides for tree leaves and atmospheric particles exhibiting the lowest ratios and highest activity.

Thus, overall data for actinide ratios are consistent with atmospheric contamination by airborne particles emitted by bauxite piles and red mud disposition units followed by their deposition on tree leaf surface at a close distance from the site. Available at a distance of greater than 1,000 m from the ponds, locally-produced foodstuffs demonstrate ^{238}U/^{232}Th close to one, suggesting that airborne micro particles emitted from the red muds disposition unit have no influence. Furthermore, the suspected influence of the soil micro particles contaminating leaf vegetables is confirmed here by the ^{238}U/^{232}Th ratio, which decreases towards one, i.e. comparable to that of the soil, when the activity of leaves increases.

Thus, the present data and especially the use of $^{238}U/^{232}Th$ have shown the influence of the Al industry on the surrounding environment. This methodology was inspired from a previous study carried out in both terrestrial and atmospheric environments of nuclear fuels facilities, where the high $^{238}U/^{232}Th$ ratio in tree leaves (1.1-14) is accounted for by the uranium released from facilities (Pourcelot et al., 2017). Both studies suggest that this activity ratio can be used to assess the potential consequences of any raw material or industrial waste in the environment as long as the ratio of these sources is known. The $^{238}U/^{232}Th$ ratio varies substantially between sources of NORM, with some enriched in ^{238}U with respect to ^{232}Th. This is particularly the case for the phosphates industry, and coal and oil mining operations, whereas other materials such as the heavy mineral industry and bauxite ore mining operations usual show the opposite ratio (Table 5). Also, potential disequilibrium between ^{238}U-decay products, as a consequence of the transformation of raw materials, may constitute an ideal tracer in the surroundings of industrial facilities (Croymans et al., 2017; Vaasma et al., 2017).

Table 5: Review of $^{238}U/^{232}Th$ (no unit) in some raw materials, industrial products, by-products and waste involving NORM.

raw materials, industrial products, by-products or waste (solid)	***$^{238}U/^{232}Th$ measurements***	***references***
phosphate minerals	10-100	Papastefanou, 2001; Guerrero et al. 2020 ; Bolivar et al. 2009
fertiliser	10-100	Baeza et al. 2011 ; Papastefanou, 2001
phosphogypsum	10	Guerrero et al. 2020
bauxite	0.3 to 1	Righi et al. 2009
bauxite	0.4	this study
red mud	0.4	this study
zircon sand	4	Righi et al. 2009
corundum	1	Righi et al. 2009
refractory products	0.9-1.2	Righi et al. 2009
coal	1-200	Lauer et al. 2019
oil shales	2.0	Vaasma et al. 2017
oil shale ashes	2.3	Vaasma et al. 2017
lignite	1-20	Hasani et al. 2014 ; Papastefanou, 2010
lignite ashes	1-20	Hasani et al. 2014

5 Conclusion

In the present study, ^{238}U, decay products and ^{232}Th in plants (tree leaves, wheat grains and leaf vegetables) were compared to the signature of atmospheric micro particles, soil and anthropogenic sources involving bauxite and red muds from the alumina industry.

Due to the low concentration of actinides usually observed in plants and atmospheric micro particles, they act as a sensitive indicator of the contribution of atmospheric particles on plant leaves, whether such particles derived from the soil (contamination of leaf vegetables) or from the aluminum industry (contamination of tree leaves). Indeed spatial and temporal variation in actinides - the mapping of ^{232}Th concentration activity in the tree leaves and day-to-day variations in the volume activity of actinides in airborne particles - have shown that a few of the samples are characterized by enhanced actinide activity. Furthermore, low $^{238}U/^{232}Th$ activity ratios in these samples show the influence of waste and raw materials from the aluminum industry as a source of actinides in the environment.

The mechanisms which enhance the uplift of red dust under the influence of wind, inducing the contamination of low atmospheric layers were not studied here, however the distance to the disposal facility and day-to-day meteorogical variations appear to be critical field parameters prone to reveal the contamination of terrestrial plants and the lower atmosphere, respectively.

6 Acknowledgements

This work was cofunded by the Labex DRIIHM, French programme "Investissements d'Avenir" (ANR-11-LABX-0010), which is managed by the ANR and by the research federation ECCOREV (CNRS-AMU). The present study benefitted from the help of foodstuff local producers who provided samples and from collaboration with people who provided plots and electric power for atmospheric micro particle sampling devices. We are also grateful to two anonymous reviewers for their useful comments. The authors warmly acknowledge Luce Evans for the edition of the English.

This work is dedicated to the memory of Catherine Cossonnet.

7 References

Anke, M., Seeber, O., Müller, R., Schäfer, U., Zerull, J., 2009. Uranium transfer in the food chain from soil to plants, animals and man. *Chem. Erde* **69**, 75-90. https://doi.org/10.1016/j.chemer.2007.12.001

Baeza, A., Corbacho, J.A., Guillén, J., Salas, A., Mora, J.C., 2011. Analysis of the different source terms of natural radionuclides in a river affected by NORM (Naturally Occurring Radioactive Materials) activities. *Chemosph.* **83**, 933-940. https://doi.org/10.1016/j.chemosphere.2011.02.042

Baskaran, M., 2011. Po-210 and Pb-210 as atmospheric tracers and global atmospheric Pb-210 fallout: A Review. *J. Environ. Radioact.* **102**, 500-513. https://doi.org/10.1016/j.jenvrad.2010.10.007

Bellis, D., Ma, R., McLeod, C.W., 2001. Characterisation of airborne uranium and thorium contamination in Northern England through measurement of U, Th and $^{235}U/^{238}U$ in tree bark. *J. Environ. Monit.* **3**, 198-201. https://doi.org/10.1039/b009220g

Bolívar, J.P., Martín, J.E., García-Tenorio, R., Pérez-Moreno, J.P., Mas, J.L., 2009. Behaviour and fluxes of natural radionuclides in the production process of a phosphoric acid plant. *Appl. Radiat. Isot.* **67**, 345-356. https://doi.org/10.1016/j.apradiso.2008.10.012

Conte, E., Widom, E., Kuentz, D., 2017. Uranium isotopes in tree bark as a spatial tracer of environmental contamination near former uranium processing facilities in southwest Ohio. *J. Environ. Radioact.* **178-179**, 265-278. https://doi.org/10.1016/j.jenvrad.2017.08.019

Croymans, T., Vandael Schreurs, I., Hult, M., Marissens, G., Lutter, G., Stroh, H., Schreurs, S., Schroeyers, W., 2017. Variation of natural radionuclides in non-ferrous fayalite slags during a one-month production period. *J. Environ. Radioact.* **172**, 63-73. https://doi.org/10.1016/j.jenvrad.2017.03.004

Ekdal, E., Karali, T., Saç, M.M., 2006. ^{210}Po and ^{210}Pb in soils and vegetables in Kucuk Menderes basin of Turkey. *Radiat. Meas.* **41**, 72-77. https://doi.org/10.1016/j.radmeas.2004.12.014

Garcia-Orellana, J., Sanchez-Cabeza, J.A., Masqué, P., Àvila, A., Costa, E., Loÿe-Pilot, M.D., Bruach-Menchén, J.M., 2006. Atmospheric fluxes of ^{210}Pb to the western Mediterranean Sea and the Saharan dust influence. *J. Geophys. Res. Atmos.* **111** (15), art. no. D15305. https://doi.org/10.1029/2005JD006660

Geagea, M.L., Stille, P., Gauthier-Lafaye, F., Millet, M., 2008. Tracing of industrial aerosol sources in an urban environment using Pb, Sr, and Nd isotopes. *Environ. Sci. Technol.* **42**, 692-698. https://doi.org/10.1021/es071704c

Goronovski, A., Vind, J., Vassiliadou, V., Panias, D., Tkaczyk, A.H., 2019. Radiological assessment of the Bayer process. *Miner. Eng.* **137**, 250-258. https://doi.org/10.1016/j.mineng.2019.04.016

Guéguen, F., Stille, P., Lahd Geagea, M., Boutin, R., 2012. Atmospheric pollution in an urban environment by tree bark biomonitoring - Part I: Trace element analysis. *Chemosph.* **86**, 1013-1019. https://doi.org/10.1016/j.chemosphere.2011.11.040

Guerrero, J.L., Pérez-Moreno, S.M., Mosqueda, F., Gázquez, M.J., Bolívar, J.P., 2020. Radiological and physico-chemical characterization of materials from phosphoric acid production plant to assess the workers radiological risks. *Chemosph.* **253**, 126682. https://doi.org/10.1016/j.chemosphere.2020.126682

Guo, G., Wu, F., Xie, F., Zhang, R., 2012. Spatial distribution and pollution assessment of heavy metals in urban soils from southwest China. *J. Envir. Sci.* **24**, 410-418. https://doi.org/10.1016/S1001-0742(11)60762-6

Hatje, V., Pedreira, R.M.A., De Rezende, C.E., Schettini, C.A.F., De Souza, G.C., Marin, D.C., Hackspacher, P.C., 2017. The environmental impacts of one of the largest tailing dam failures worldwide. *Sci. Rep.* **7**, 10706. https://doi.org/10.1038/s41598-017-11143-x

Hasani, F., Shala, F., Xhixha, G., Xhixha, M.K., Hodolli, G., Kadiri, S., Bylyku, E., Cfarku, F., 2014. Naturally occurring radioactive materials (NORMs) generated from lignite-fired power plants in Kosovo. *J. Environ. Radioact.* **138**, 156-161. https://doi.org/10.1016/j.jenvrad.2014.08.015

Hissler, C., Stille, P., Krein, A., Geagea, M.L., Perrone, T., Probst, J.-L., Hoffmann, L., 2008. Identifying the origins of local atmospheric deposition in the steel industry basin of Luxembourg using the chemical and isotopic composition of the lichen Xanthoria parietina. *Sci. Tot. Envir.* **405**, 338-344. https://doi.org/10.1016/j.scitotenv.2008.05.029

IAEA, 2017. The environmental behaviour of polonium, Technical reports series no. 484, ISSN 0074–1914, International Atomic Energy Agency, Vienna.

Jeambrun, M., Pourcelot, L., Mercat, C., Boulet, B., Pelt, E., Chabaux, F., Cagnat, X., Gauthier-Lafaye, F., 2012. Contribution of uranium, thorium and decay products in soil, water and atmospheric particles, to the activity concentration in lettuce and wheat samples. *J. Environ. Monit.* **14**, 2902-2912. https://doi.org/10.1039/C2EM30434A

Karagiannidi, Th., Papaefthymiou, H., Papatheodorou, G., 2009. Radioactive impact of a bauxite beneficiation plant in the Itea Gulf (Gulf of Corinth, Greece). *J. Radioanal. Nucl. Chem.* **279**, 923-934. https://doi.org/10.1007/s10967-008-7412-3

Lasalle, J-L, Malfait, Ph., 2017. Impact sanitaire du site de stockage de Mange-Garri, rapport Santé Publique France Etudes et Enquêtes, 43 p.

Lauer, N., Vengosh, A., Dai, S., 2017. Naturally Occurring Radioactive Materials in Uranium-Rich Coals and Associated Coal Combustion Residues from China. *Environ. Sci. Technol.* **51**, 13487-13493. https://doi.org/10.1021/acs.est.7b03473

Lindahl, P., Maquet, A., Hult, M., Gasparro, J., Marissens, G., González de Orduña, R., 2011. Natural radioactivity in winter wheat from organic and conventional agricultural systems. *J. Environ. Radioact.* **102**, 163-169. https://doi.org/10.1016/j.jenvrad.2010.11.007

McDonald, P., Jackson, D., Leonard, D.R.P., McKay, K., 1999. An assessment of ^{210}Pb and ^{210}Po in terrestrial foodstuffs from regions of England and Wales. *J. Environ. Radioact.* **43**, 15-29.

Papastefanou, C., 2001. Radiological impact from atmospheric releases of ^{238}U and ^{226}Ra from phosphate rock processing plants. *J. Environ. Radioact.* **54**, 75-83. https://doi.org/10.1016/S0265-931X(00)00167-3

Papastefanou, C., 2010. Escaping radioactivity from coal-fired power plants (CPPs) due to coal burning and the associated hazards: A review. *J. Environ. Radioact.* **101**, 191-200. https://doi.org/10.1016/j.jenvrad.2009.11.006

Pietrzak-Flis, Z., Skowrońska-Smolak, M., 1995. Transfer of ^{210}Pb and ^{210}Po to plants via root system and above-ground interception. *Sci. Tot. Environ.* **162**, 139-147.

Pietrzak-Flis, Z., Suplinska, M.M., Rosiak, L., 1997. The dietary intake of ^{238}U, ^{234}U, ^{230}Th, ^{232}Th, ^{228}Th and ^{226}Ra from food and drinking water by inhabitants of the Walbrzych region. *J. Radioanal. Nucl. Chem.* **222**, 189-193.

Pourcelot, L., Boulet, B., Le Corre, C., de Vismes Ott, A., Cagnat, X., Cossonnet, C., Thomas, S., Loyen, J., Fayolle, C., Van Hecke, W., Martinez, B., Petit, J., Kaltenmeier, R., Gieré, R., 2011. Actinides and decay products in some foodstuff and bioindicators in the surrounding an uranium plant. *J. Environ. Monit.* **13**, 1327-1336. https://doi.org/10.1016/j.jenvrad.2017.02.001

Pourcelot, L., Masson, O., Renaud, P., Cagnat, X., Boulet, B., Cariou, N., De Vismes-Ott, A., 2015. Environmental consequences of uranium atmospheric releases from fuel cycle facility: II. The atmospheric deposition of uranium and thorium on plants. *J. Environ. Radioact.* **141**, 1-7. https://doi.org/10.1016/j.jenvrad.2014.11.018

Pourcelot, L., Masson, O., Saey, L., Conil, S., Boulet, B., Cariou, N., 2017. Empirical calibration of uranium releases in the terrestrial environment of nuclear fuel cycle facilities. *J. Environ. Radioact.* **171**, 74-82. https://doi.org/10.1016/j.jenvrad.2017.02.001

Righi, S., Verità, S., Albertazzi, A., Rossi, P.L., Bruzzi, L., 2009. Natural radioactivity in refractory manufacturing plants and exposure of workers to ionising radiation. *J. Environ. Radioact.* **100**, 540-546. https://doi.org/10.1016/j.jenvrad.2009.03.008

Rihs, S., Prunier, J., Thien, B., Lemarchand, D., Pierret, M.-C., Chabaux, F., 2011. Using short-lived nuclides of the U- and Th-series to probe the kinetics of colloid migration in forested soil. *Geochim. Cosmochim. Acta* **75**, 7707-7724. https://doi.org/10.1016/j.gca.2011.09.045

Sheppard, S.C., Sheppard, M.I., Ilin, M., Tait, J., Sanipelli, B., 2008. Primordial radionuclides in Canadian background sites: secular equilibrium and isotopic differences. *J. Environ. Radioact.* **99**, 933-946. https://doi.org/10.1016/j.jenvrad.2007.11.018

Segura, F.R., Nunes, E.A., Paniz, F.P., Paulelli, A.C.C., Rodrigues, G.B., Braga, G.U.L., Pedreira Filho,W.R., Barbosa Jr., F., Cerchiaro, G., Silva, F.F., Batista, B.L., 2016. Potential risks of the residue from Samarco'smine damburst (Bento Rodrigues, Brazil). *Environ. Pollut.* **218**, 813-825. https://doi.org/10.1016/j.envpol.2016.08.005

Tortorello, R., Widom, E., Renwick, W.H., 2013. Use of uranium isotopes as a temporal and spatial tracer of nuclear contamination in the environment. *J. Environ. Rad.* **124**, 287-300. https://doi.org/10.1016/j.jenvrad.2013.06.007

Turtiainen, T., Kostiainen, E., Hallikainen, A., 2011. ^{210}Pb and ^{210}Po in Finnish cereals. *J. Environ. Radioact.* **102**, 438-442. https://doi.org/10.1016/j.jenvrad.2010.09.009

Vaasma, T., Loosaar, J., Kiisk, M., Tkaczyk, A.H., 2017. Radionuclide concentration variations in the fuel and residues of oil shale-fired power plants: Estimations of the radiological characteristics over a 2-year period. *J. Environ. Radioact.* **173**, 25-33. https://doi.org/10.1016/j.jenvrad.2016.10.005

Zhang, Y., Wang, X., Chen, H., Yang, X., Chen, J., Allen, J.O., 2009. Source apportionment of lead-containing aerosol particles in Shanghai using single particle mass spectrometry. *Chemosph.* **74**, 501-507. https://doi.org/10.1016/j.chemosphere.2008.10.004

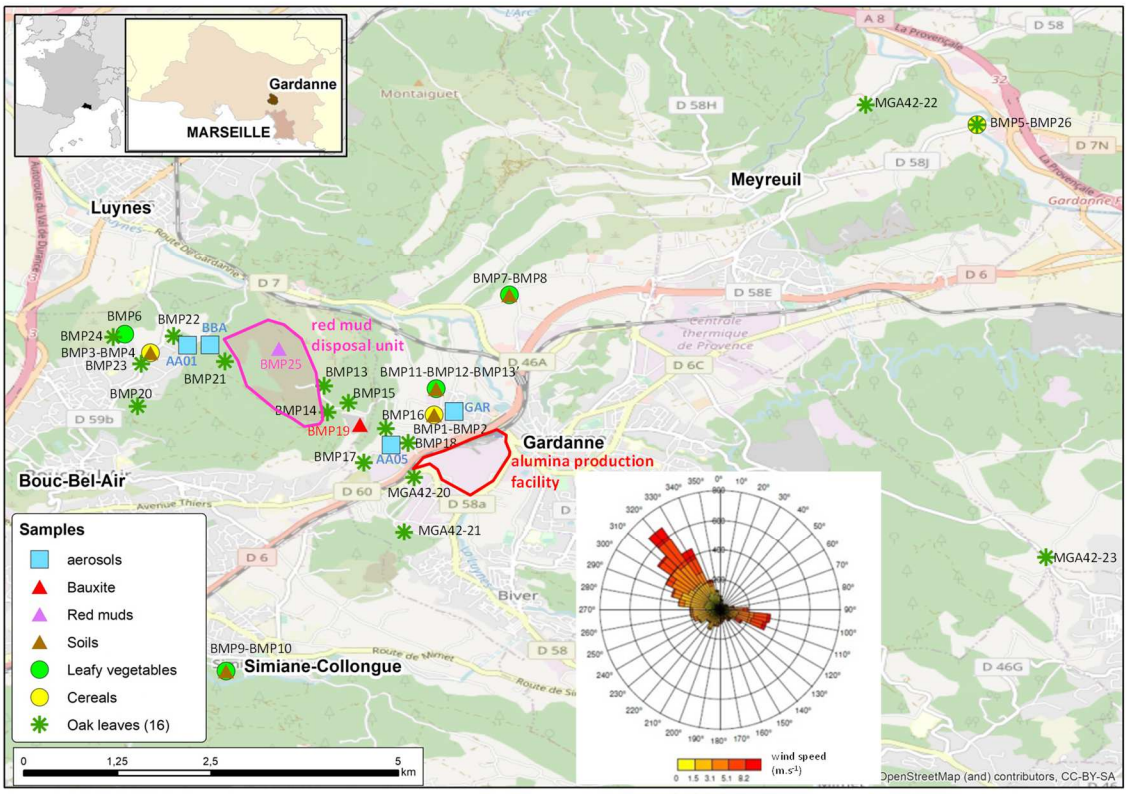

Figure 1: location of sampling sites and main winds (Météo-France data) in the environment of the alumina production facility and the red mud disposition site at Mange Garri.

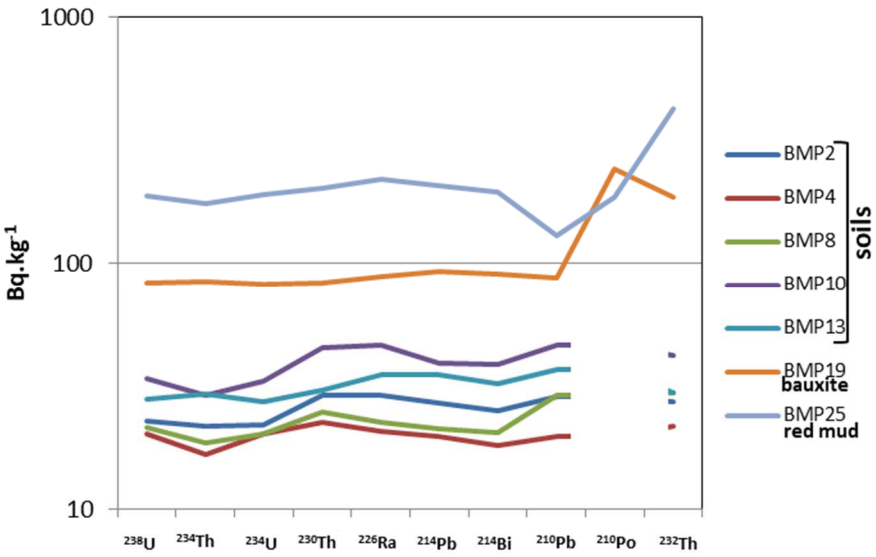

Figure 2: concentration activity of radionuclides in soil, bauxite and red mud samples (Bq kg^{-1}).

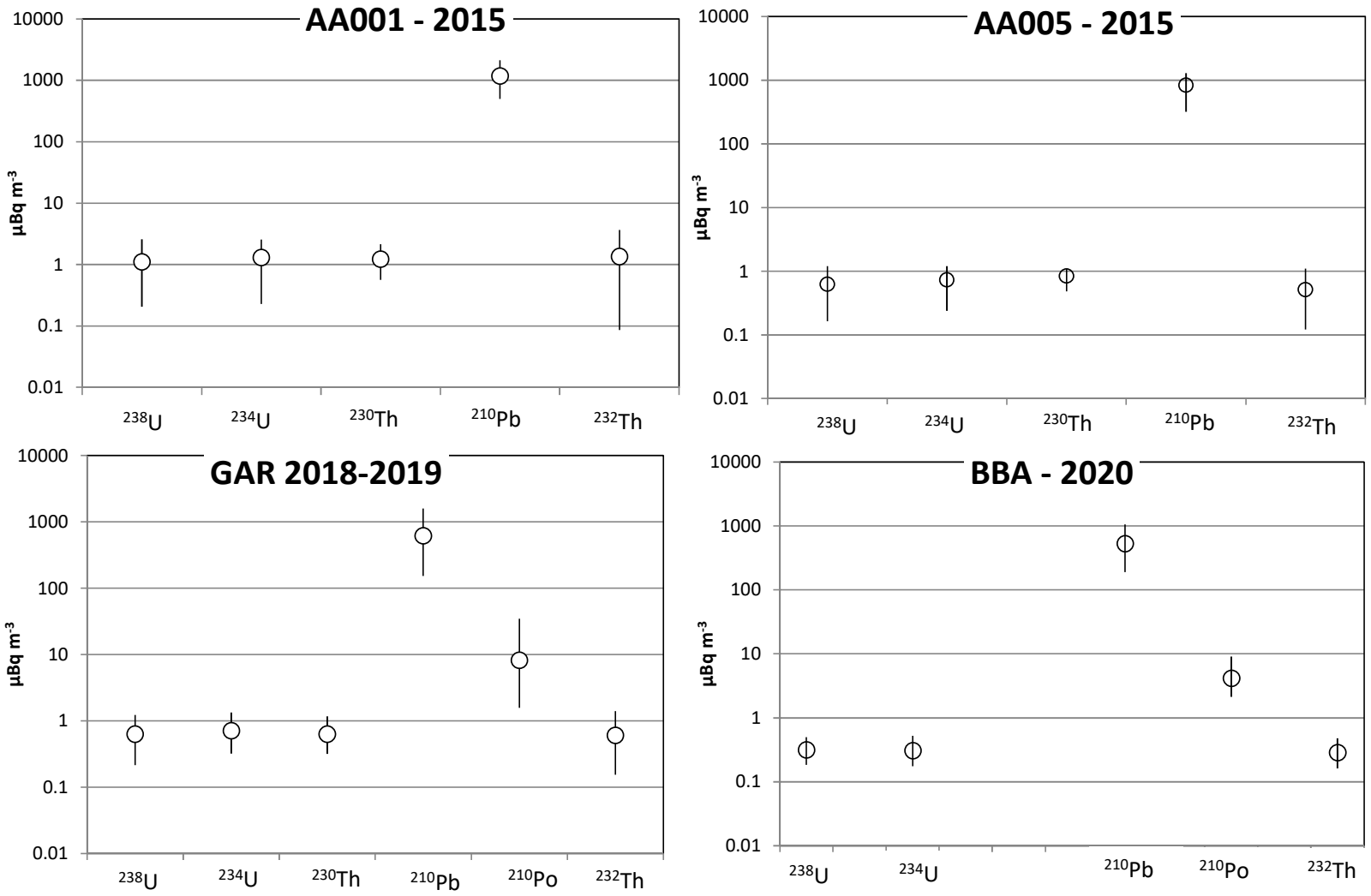

Figure 3: Mean, maximum and minimum volume activity of NORM in atmospheric micro particle samples taken W (AA001 and BBA) and E (AA005 and GAR) of the red mud disposition unit (µBq m^{-3}).

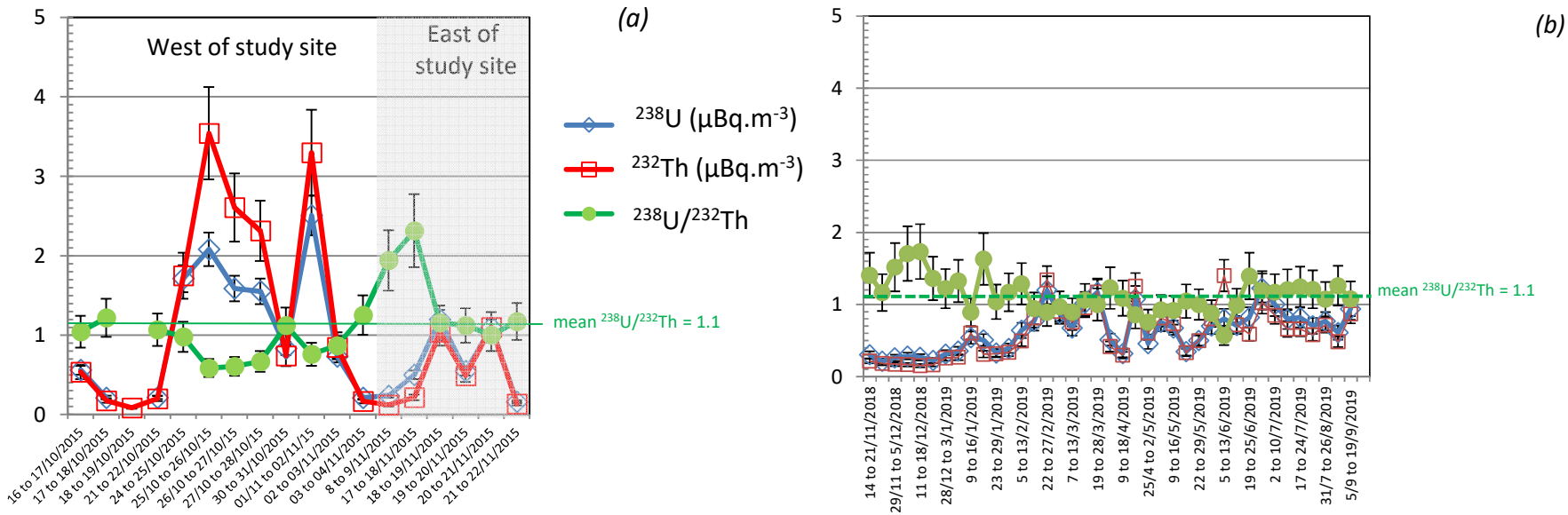

Figure 4: Daily volume activity of ^{238}U, ^{232}Th (µBq m^{-3}) and activity ratio $^{238}U/^{232}Th$, in 2015 (a) and in 2018-2019 (b).

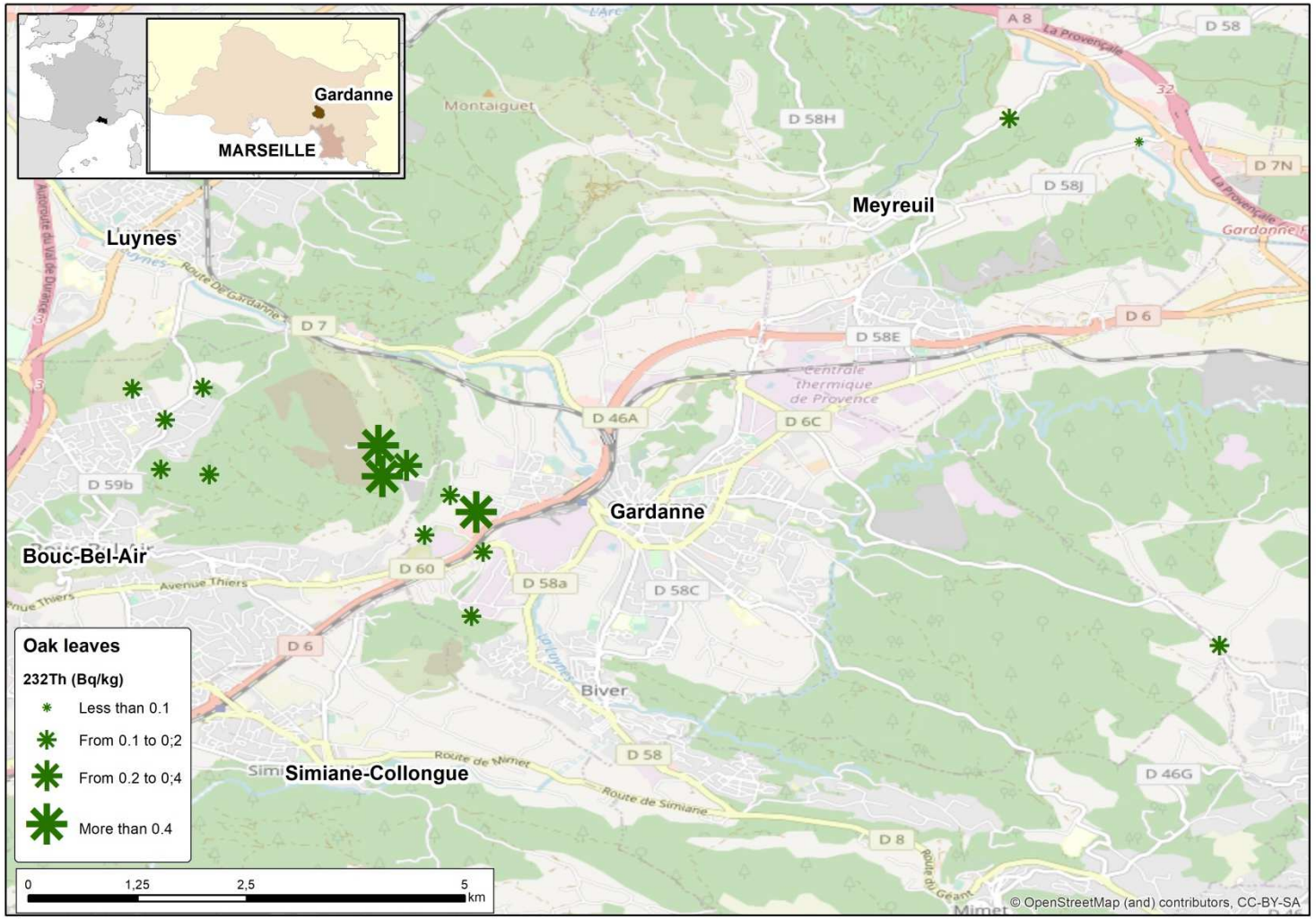

Figure 5: Map of ^{232}Th concentration activity in oak leaf samples (Bq kg^{-1}).

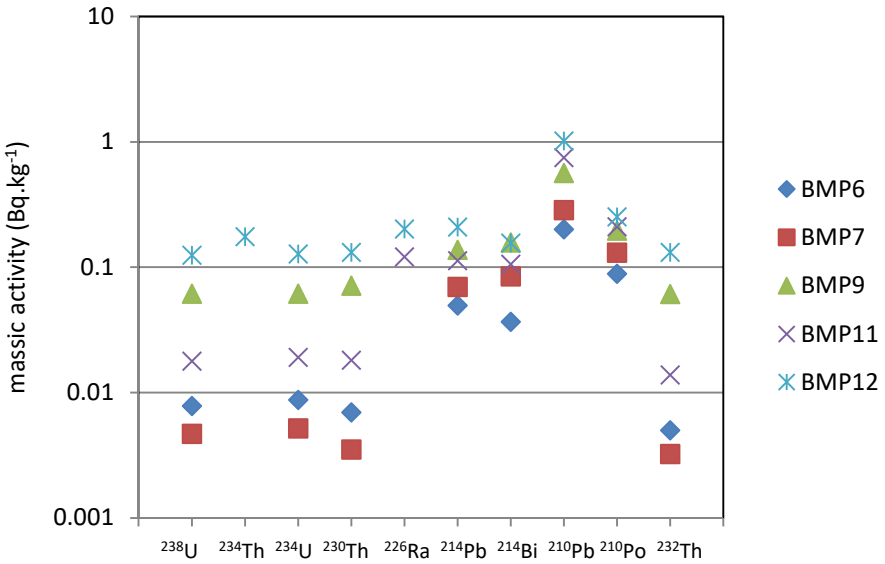

Figure 6: radionuclide concentration activity in leaf vegetables samples (Bq kg^{-1} fresh weight).

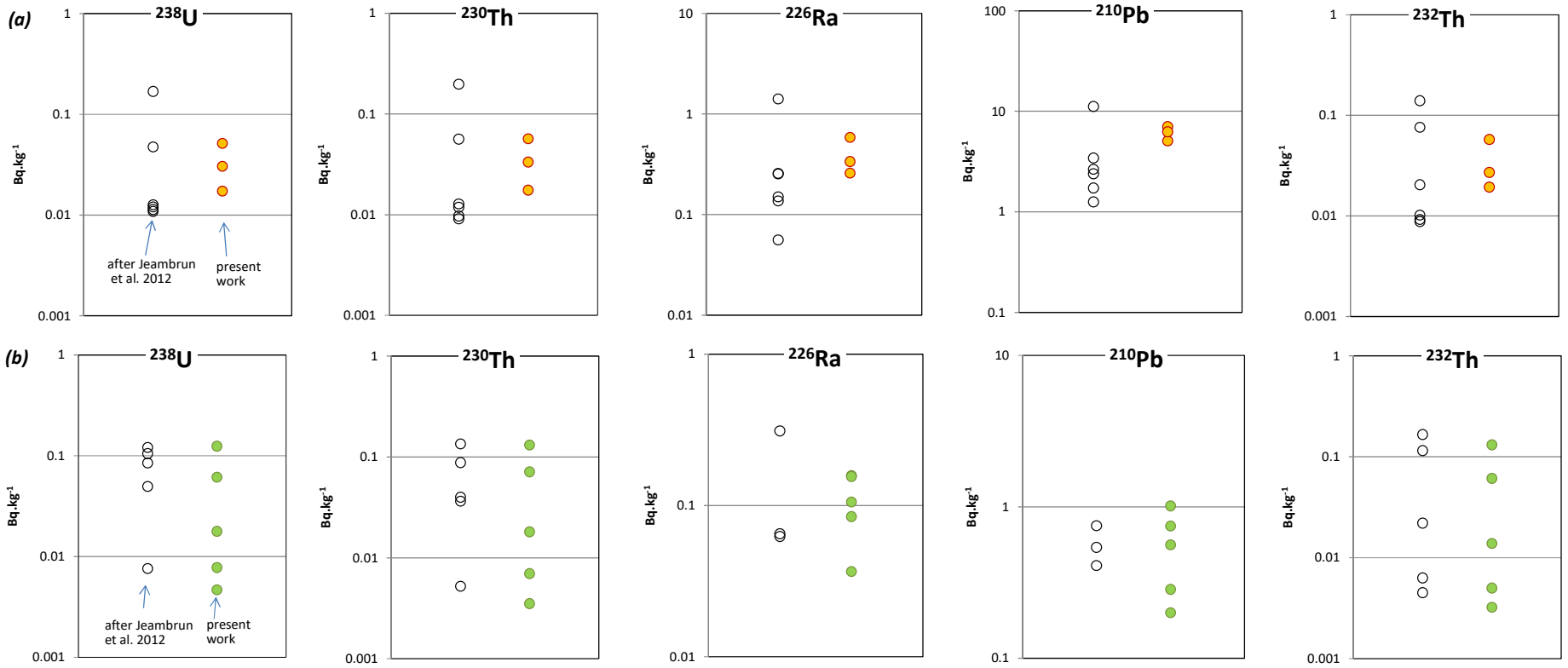

Figure 7: Concentration activity of ^{238}U, some decay products and ^{232}Th (a) in wheat grain samples and (b) in leaf vegetable samples. Present work data are compared to data acquired in the same foodstuff products sampled over France (after Jeambrun et al., 2012).

(a)

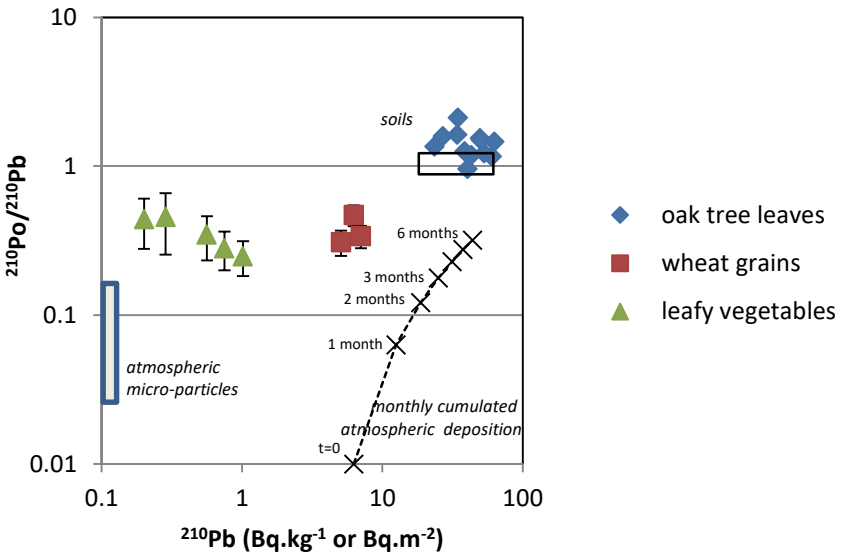

(b)

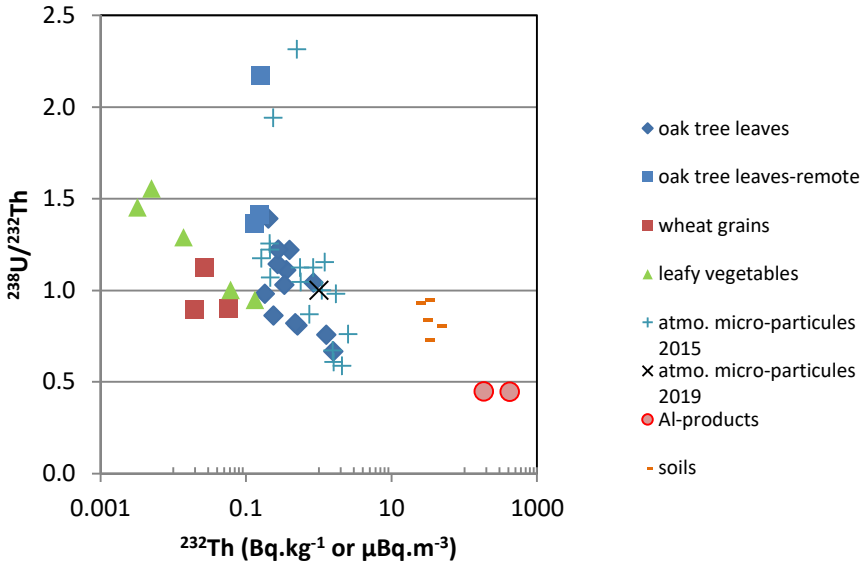

Figure 8: (a) ^{210}Po/^{210}Pb vs ^{210}Pb activity and (b) ^{238}U/^{232}Th vs ^{232}Th concentration activity in the plants studied compared to some of the potential sources of radionuclides (atmospheric micro-particles, soils, and Al products).